NASA TECHNICAL MEMORANDUM

NASA TM X-52874

NASA TM X-52874

EMPIRICAL CORRELATION OF SMALL HOLLOW SPHERE IMPACT FAILURE DATA USING DIMENSIONAL ANALYSIS

by Richard E. Morris
Lewis Research Center
Cleveland, Ohio
September 1970

This information is being published in preliminary form in order to expedite its early release.

ABSTRACT

Correlation equations were obtained for published experimental small hollow sphere-impact data. The failure deformation (δ_f) as a function of mean radius (R), thickness (h), and ultimate strain (ϵ) is given by

$$\delta_f/R = 0.109\ (R/h)^{0.64}\ \epsilon^{\frac{1}{2}}$$

The failure velocity (V_f) as a function of mean radius, thickness, ultimate stress (σ), density (ρ), and ultimate strain (ϵ) is given by

$$V_f = 0.15\ (R/h)^{0.56}\ (\sigma/\rho)^{\frac{1}{2}}\ \epsilon^{\frac{1}{2}}$$

Sphere materials included SAE 4130 steel, titanium, and Haynes Alloy No. 25. Diameters varied from 0.750 to 2.000 inches (1.91 to 5.08 cm). Failure velocities varied from 297 to 650 ft/sec (91 to 198 m/sec).

The correlation equations were used to calculate the failure velocity and deformation of a 17 ft. (5.18 m) diameter containment vessel for a nuclear reactor. The deformation at failure was 7.0 ft. (2.13 m) at an impact velocity of 900 ft/sec (274 m/sec).

The equations indicate that a multilayer spherical containment vessel probably would have greater impact strength than a corresponding single wall vessel.

EMPIRICAL CORRELATION OF SMALL HOLLOW SPHERE IMPACT FAILURE DATA USING DIMENSIONAL ANALYSIS

by

Richard E. Morris

Lewis Research Center
National Aeronautics and Space Administration
Cleveland, Ohio

E-5907

SUMMARY

Published experimental sphere impact data were analyzed to determine the effects of sphere radius, thickness, material, and impact velocity on the impact deformation and failure of hollow spherical shells moving normal to and impacting on a hard flat surface. The information is needed to predict the effect of impact on a nuclear reactor containment vessel 10 to 20 feet (3.05 to 6.10 m) in diameter with a wall thickness of about 3 inches (7.62 cm). A method was needed for extrapolating from the small hollow sphere impact test data to predict the effects of impact on large spherical containment vessels.

Dimensional analysis was used to obtain correlating equations for small sphere data. Outside diameters of spheres were 0.750 to 2.000 inches (1.91 to 5.08 cm). Deformation was defined by the radial distance the impact surface of the sphere was permanently deflected toward the center of the sphere. Failure velocities varied from 297 to 650 ft/sec (91 to 198 m/sec). Spheres were fabricated from SAE 4130 steel, titanium, and Haynes Alloy No. 25.

One equation states that the failure deformation-to-radius ratio (δ_f/R) increases with the radius-to-thickness ratio (R/h), and with the ultimate strain (ϵ).

$$\frac{\delta_f}{R} = 0.109 \left(\frac{R}{h}\right)^{0.64} \epsilon^{\frac{1}{2}} \tag{1}$$

Another equation shows that the failure velocity (V_f) increases with the radius-to-thickness ratio, with the ultimate stress-to-density ratio (σ/ρ), and with the ultimate strain.

$$V_f = 0.163 \, (R/h)^{0.56} \, (\sigma/\rho)^{\frac{1}{2}} \, \epsilon^{\frac{1}{2}} \tag{2}$$

X-52874

The standard deviation of the experimental failure velocities from values given by the correlating equation is 20 percent. Thus, 68 percent of the experimental failure velocities would be expected to fall within a band of ±20 percent from correlation equation values.

The equations show that both the failure deformation and the failure velocity are strongly dependent on the mean radius to thickness ratio. Variation of either the mean radius or the thickness to give a higher value for the ratio will increase both the failure velocity and the deformation at failure. The correlation equations also indicate that a multilayer containment vessel should have a significantly higher failure velocity than a single layer containment vessel of the same total thickness because thin wall vessels yield a higher failure velocity.

These equations were used to calculate the failure velocity and deformation of a 17 ft. (5.18 m) diameter, 3 in. (7.62 cm) wall, Type 304 stainless steel containment vessel for a nuclear reactor. The deformation for failure was 7.0 ft. (2.13 m) at an impact velocity of 900 ft/sec (274 m/sec).

Hollow sphere impact tests are needed to verify the correlation equations. The tests should be designed to investigate the effect of larger diameters and the effect of multilayer wall spherical shells on impact deformation and failure.

INTRODUCTION

Safety is a primary requirement in the design of a nuclear airplane. The importance of safety with regard to nuclear aircraft has been discussed in reference 1. Release of radioactive fission products to the atmosphere in the event of a crash landing must be prevented. One method of preventing fission product release is to enclose the reactor in a containment vessel. Valve closures would be provided to completely seal the containment vessel in an emergency such as a crash landing of the airplane.

The radioactive contents of the containment vessel must remain sealed in the vessel even though the vessel is deformed by an impact. Afterheat from the nuclear reactor will heat the deformed containment vessel and raise internal vapor pressure. Then in the heated, deformed condition, pressure generated inside the containment vessel must be contained.

The containment vessel for an aircraft nuclear reactor will be a relatively large sphere approximately 10 to 20 feet (3.05 to 6.10 m) in diameter, with a wall thickness of approximately 3 inches (7.62 cm). The containment vessel material must have high strength to resist impact deformation and must also have sufficient ductility to allow for impact deformation without rupture.

Impact energy absorbers may be provided to absorb part of the impact energy of the containment vessel package. The amount of energy absorbers that can be designed to protect the containment vessel (as described in reference 2) is limited by the weight of the energy absorbers. Complete protection of the containment vessel would require so much energy absorber that the added weight may be too great for an airborne system. Thus, part of the kinetic energy of the containment vessel package must be absorbed in the deformation of the containment vessel.

The relations for impact deformation with and without rupture must be known for large spheres in order to design the containment vessel to withstand impact without rupture. In reference 3, small sphere deformation data was extrapolated to large spheres by correlating data from small hollow spheres that deformed during impact without rupture. The purpose of this report is to correlate small sphere impact data at rupture and to predict the deformation and impact velocity at failure for large hollow spheres such as a containment vessel.

The impact of spherical shells is a subject of relatively recent theoretical and experimental interest. Simonis and Stoneking (ref. 4) presented their work on the impact of spherical shells in December 1966. Haskell (ref. 5) presented a failure criterion for spherical shells in December 1968. He used the experimental sphere impact data reported by Simonis and Stoneking in reference 4.

An attempt was made to apply the Haskell criterion (ref. 5) for the impact failure of spherical shells to a large containment vessel. The failure velocity obtained was unreasonably low. The criterion was based on sphere impact tests of Simonis and Stoneking using spheres with diameters of 0.750 to 1.250 inches (1.91 to 3.18 cm). Haskell's empirical criterion could not be extrapolated for use in the design of a large containment vessel.

Reference 6 gives recent test data on the impact of spherical shells. The 4.00 inch (10.16 cm) diameter spheres tested are the largest diameter hollow spheres for which test data was available. Failures occurred during 2 inch (5.08 cm) diameter sphere impact tests. None of the 4 inch (10.16 cm) diameter spheres failed in the tests.

Johnson (ref. 7) obtained solutions for the impact of an elastic spherical shell on an elastic surface. His solutions as well as those of Simonis and Stoneking make the assumption of small deflections. Analyses based on small deflection theory cannot describe the impact of spheres undergoing large permanent deformations. Consequently, no available theoretical analysis was applicable to the problem of calculating failure velocity or failure deformation.

SYMBOLS

a	Constant
b	Constant
c	Constant
h	Wall Thickness, in., cm
k	Constant
k'	Constant
m	Constant
n	Constant
N	Percent Failures at a Given Velocity
R	Mean Radius of Hollow Sphere, in., cm
V	Impact Veloicty, ft/sec, m/sec
ϵ	Ultimate True Strain, in./in., cm/cm
δ	Deformation, in., cm
ρ	Density of Sphere Material, lbm/in^3, g/cm^3
σ	Ultimate Stress, psi, MN/m^2
Ø	Angle

Subscript

f	Failure Due to Rupture

ANALYSIS

In the absence of an analytical or empirical method of predicting the failure velocity or deformation of large hollow spheres, the available experimental hollow sphere impact data (refs. 4 and 6) were studied using dimensional analysis.

Dimensional Analysis

R	Mean Radius of Hollow Sphere	L
h	Wall Thickness	L
ρ	Density of Sphere Material	$M\ L^{-3}$
σ	Ultimate Stress	$M\ L^{-1}\ T^{-2}$
V_f	Failure Velocity	$L\ T^{-1}$
ϵ	Ultimate True Strain	
δ_f	Deformation, Radial Deflection of Impact Surface at Failure	L

There are seven variables (R, h, ρ, σ, V_f, ϵ, δ_f) and three dimensions (L, M, T). Dimensional analysis yields four dimensionless pi ratios.

$$\pi_1 = \frac{\rho V^2}{\sigma} \qquad \pi_2 = \frac{\delta_f}{R}$$

$$\pi_3 = \frac{R}{h} \qquad \pi_4 = \epsilon$$

The deformation-radius ratio (δ_f/R) can be expressed as a function of the other three ratios.

$$\frac{\delta_f}{R} = K\left(\frac{\rho V^2}{\sigma}\right)^a \left(\frac{R}{h}\right)^b \epsilon^c \tag{3}$$

The ratio, δ/R, is a measure of the severity of the deformation of the hollow sphere. It is proportional to the angle $\emptyset$ between a radial line drawn perpendicular to the flattened impact surface and a radius drawn to the intersection of the undeformed surface and the flattened surface of the sphere (see fig. 1). This angle is related to the severity of the bending or shear deformation at the periphery of the flattened surface.

Equation (4) was presented in reference 3. This is a general equation relating deformation and impact velocity below the failure velocity.

$$\delta/R = 0.67 \left(\frac{\rho V^2}{\sigma}\right)^{\frac{1}{2}} \left(\frac{R}{h}\right)^{0.08} \qquad (4)$$

Symbols for deformation and velocity without the subscript f refer to velocities and deformations from spheres tested without failure. The equation was obtained using dimensional analysis. It agrees with the conclusion of Simonis and Stoneking (ref. 4) that the change in diameter of impacted spheres was a linear function of the impact velocity.

The failure velocity used in this analysis is defined as the lowest test velocity that resulted in a through-crack in the wall of the test sphere. At high strain rates, the average dynamic stress associated with plastic flow of the sphere material is assumed to approach the ultimate strength of the material. Therefore, the ultimate strength of sphere materials is used in this analysis.

Figure 1 is a plot of equation (4) using the data from tables 1 and 2 for failed spheres. The solid line is a graph of the equation. The fit of the experimental deformation-radius ratios for the failed spheres to the empirical equation is essentially similar to the fit of experimental data from unfailed hollow sphere impacts shown in reference 3. There is no evidence in figure 1 to show that the deformation-radius ratios obtained from failed spheres was affected by the cracks in the walls of the spheres. Consequently the range of application of equation (4) can be extended to include deformation-radius ratios for sphere impacts at failure velocities.

Equation (3) differs from equation (4) in that equation (4) is a general deformation correlation equation whereas equation (3) is an equation for that particular deformation-radius ratio at which failure will occur. The same variables are present in both relations except for the ultimate strain.

Equation (3) has three exponents to be evaluated. At the failure velocity, the deformation-radius ratio is the same for both equations (3) and (4). Equating the two equations eliminates the failure deformation-radius ratio yielding an equation in three dimensionless ratios. This equation may be solved for $(\rho V_f^2/\sigma)^{\frac{1}{2}}$. Substitution of k' for the numerical coefficient and replacing the algebraic exponents with m and n gives equation (5).

$$\left(\frac{\rho V_f^2}{\sigma}\right)^{\frac{1}{2}} = k' \left(\frac{R}{h}\right)^m \epsilon^n \qquad (5)$$

The ultimate strain has the same value for all specimens from a given material. Consequently the right side of equation (5) becomes a constant times the exponential function of R/h for a given material. The log-log plot of equation (5) provides a family of lines having a slope equal to m. Data from each set of specimens having a fixed value for ultimate strain will plot as one line on the graph.

There are 11 data points. Three materials are represented. However, there is only one data point per material for two of the materials tested. A line was drawn through the nine data points for SAE 4130 specimens in a graph of equation (5). Parallel lines were drawn through the Haynes Alloy No. 25 and the Titanium data points. Data for constant values of R/h were obtained from the graph. A graph of equation (5) with R/h constant was plotted to obtain a value for n. The slope (n) of the line through the three noncollinear points could not be evaluated precisely but the value of n = 0.5 was chosen for a reasonable data fit. This value improved the fit of the titanium and the Haynes Alloy sphere impact data points on graphs of data.

Figure 2 shows a graph of R/h versus $(\rho/\sigma)^{\frac{1}{2}} V_f/\epsilon^{\frac{1}{2}}$. The solid line is the least squares regression of R/h on $(\rho/\sigma)^{\frac{1}{2}} V_f/\epsilon^{\frac{1}{2}}$. Equation (6) is the equation of the solid line in figure 2. This equation provides values for k' and m in equation (5).

$$\left(\frac{\rho}{\sigma}\right)^{\frac{1}{2}} \frac{V_f}{\epsilon^{\frac{1}{2}}} = 0.163 \left(\frac{R}{h}\right)^{.560} \tag{6}$$

Equation (6) may be solved for V_f.

$$V_f = 0.163 \left(\frac{R}{h}\right)^{.560} \left(\frac{\sigma\epsilon}{\rho}\right)^{\frac{1}{2}} \tag{7}$$

Substitution for V_f from equation (7) into equation (4) yields the equation for the failure deformation-radius ratio.

$$\frac{\delta_f}{R} = 0.109 \left(\frac{R}{h}\right)^{0.64} \epsilon^{\frac{1}{2}} \tag{8}$$

An equation for the failure deformation-thickness ratio is obtained by multiplying equation (8) by R/h.

$$\frac{\delta_f}{h} = 0.109 \left(\frac{R}{h}\right)^{1.64} \epsilon^{\frac{1}{2}} \tag{9}$$

Figures 3, 4, and 5 are graphs of equations (7), (8), and (9).

Equation (8) corresponds to equation (3). The constant k in equation (3) has the value 0.109. The kinetic energy to ultimate stress ratio dropped out when the expression for failure velocity was substituted into the general deformation-radius equation (4). Hence, the exponent a = 0. The exponent b = 0.64. And the exponent c = 0.50.

RESULTS

Hollow sphere impact failure test data obtained from published references was analyzed using dimensional analysis. Failure velocity for a given sphere geometry and material was selected from the impact test data as the lowest impact test velocity that resulted in failure of the sphere. Failure was defined by the presence of a through-crack in the wall of the impacted sphere.

The range of the failed sphere data is as follows: The failure velocity varied from 297 to 650 feet per second (91 to 198 m/sec). Sphere geometries ranged from thick-walled to thin-walled spheres. Mean radius to thickness ratios of sphere test data varied from 2.9 to 28.1. Outside diameters ranged from 0.750 to 2.00 inches (1.91 to 5.08 cm). Materials included SAE 4130 steel and titanium spheres tested at room temperature, and Haynes Alloy No. 25 spheres tested at 1800°F (1256°K).

Empirical correlation equations presented can be used to predict the permanent deformation and the impact velocity which will cause failure of a hollow sphere moving normal to and impacting on a hard flat surface.

The general hollow sphere impact deformation equation presented in reference 3 was found to be applicable to hollow sphere impact failure test data. The ratio of deformation at failure to sphere radius or thickness was found to be independent of impact velocity, density of the sphere material, and the ultimate stress parameters. As shown by equations (8) and (9), both ratios correlated with functions only of geometry and ultimate strain.

Equation (7), an empirical correlation equation for failure velocity, was found to be a function of geometry and materials properties. The equation presented states that the failure velocity is proportional to the mean radius-to-thickness ratio to the 0.56 power, to the square root of the ultimate stress times the ultimate true strain, and is inversely proportional to the square root of the density of the sphere material.

The standard deviation of the experimental failure velocities from correlation equation (equation 7) values is 20 percent. Thus assuming a normal distribution due to random data scatter, 68 percent of the experimental hollow sphere impact failure velocities would be expected to fall within a band of ±20 percent from the correlation equation values.

DISCUSSION OF RESULTS

This section of the report includes a discussion of the correlation equations and the fit of the experimental data. Sources of variation of the data points from the correlation include the method of determining the failure velocity and the consequent variation in the probability of failure associated with each of the data points.

Another source of variation is the uncertainty or lack of information concerning the dynamic properties of the sphere materials. The specific energy of a material is equal to the area under the dynamic true-stress versus true-strain diagram. This property is an important parameter of the impact failure velocity.

Limitations of the correlation equations are discussed. Effects of variation of the parameters are interpreted to suggest that a hollow sphere with a multilayer wall would have a superior impact strength.

Finally, application of the correlation equations to the impact of a large spherical containment vessel provided evidence that such a vessel can sustain considerable deformation at relatively high velocities without failure.

Correlation Equations

Figures 3 to 5 are graphs of the failure deformation and failure velocity correlation equations (7) to (9). The solid lines are graphs of the equations. The dashed lines define ranges of ± 30 percent based on the ordinate functions. In figure 3 the standard deviation (s) is given as 20 percent. Hence the dashed lines define a band of ± 1.5 standard deviations. Eighty-seven percent of the experimentally determined failure velocities would be expected to fall within the region defined by the dashed lines.

Each of the graphs shows scattering of the experimental data about the solid correlation line. The failure deformation to thickness ratio in figure 5 has the greatest range of variation of the 11 experimental data points. This graph verifies that the correlation equation is representative of the failure deformation behavior of the experimental sphere impact test data.

The scatter of the data points in figures 3 and 4 suggests that there might be some sources of variation other than the random variation of the variables in the correlation equations.

Sources of Variation of Experimental Data

Important sources of variation of the experimental data include the procedure for the determination of the failure velocity and the methods for controlling and determining materials properties.

Determining the failure velocity.- The procedure for determining the failure velocity was an important source of variation in the experimental failure velocity data. The lowest impact test velocity that resulted in a through-crack in the wall of the sphere of a given geometry and material was selected as the failure velocity.

The experimental impact tests of Simonis and Stoneking (ref. 4) verify that there is a range of impact velocity between the velocity with a very small probability of failure and the velocity with a very small probability of surviving the impact (non-failure).

As shown in figure 6, when the impact velocity is below some value there will be a region of no failures. As the impact velocity is increased, there is a velocity above which all specimens will fail on impact. That is, the probability of failure is 100 percent. A plot of the rate of change in percent failures at a given velocity (dN/dV) versus impact velocity is also shown in figure 6. At some velocity 50 percent of the impact specimens will fail. At that velocity, the rate of change in percent failures is zero. As velocity increases above the value for 50 percent failures, the rate of change in percent failures decreases and falls to zero.

Assume that dN/dV is normally distributed about the impact velocity with a 50 percent probability of failure. The curve can then be normalized so that the area under the curve is equal to one. At an impact velocity which is three standard deviations (3s) less than the velocity for 50 percent failures, there is a very small probability of failure. At an impact velocity which is three standard deviations (3s) greater than the velocity for 50 percent failures, there is almost a 100 percent probability of failure.

Reference 4 provides an extensive report on a large number of sphere impact tests. In one series of tests of one geometry, most of the test velocities were in the region of 100 percent failures (see fig. 6). Sixteen out of 19 test spheres failed om impact. All of the 19 spheres impact velocities were greater than the 50 percent failure velocity. Consequently the failure velocity reported for that set of tests has more than a 50 percent probability of failure.

A study of the frequency of failure versus velocity plots for each set of data showed that some of the experimental failure velocities would fall above and some would fall below the 50 percent failure velocity. The correlation equation for failure velocity is the equation for a

line developed to fit the experimental data points. Thus, the failure velocity correlation equation will give values of failure velocity that fall near the center of the probability distribution. And the correlation equation gives values for failure velocity with approximately a 50 percent probability of failure.

Because of the method of selection, experimental failure velocities do not have a uniform probability of failure. Variation in the probability of failure of the experimental failure velocity data contributes to the scatter in figure 3 and in the other graphs of data.

One objective of future sphere impact tests should be to establish sphere impact failure velocities with a uniform level of probability. The test program may be designed to provide the number of experimental sphere impacts required to get the selected level of probability.

Materials properties.- The behavior of spheres under conditions of impact deformation and failure are dependent upon the dynamic properties of the sphere materials. No dynamic property data is available for the materials used to fabricate the test spheres. Consequently some assumptions were necessary.

The average dynamic plastic flow stress of the hollow sphere materials was assumed to approach the ultimate strength. The ultimate strength was used in the analysis. The dynamic ultimate true strain associated with failure of impact deformed spheres was assumed to be the ultimate true strain obtained from static tensile tests based on the reduction of area. In the case of Haynes Alloy No. 25, the ultimate true strain was based on the reduction in area of a static tensile specimen of cast bar that was tested at 1800°F (1256°K) (ref. 8) since that was the best value available. Values used for ultimate strength and ultimate true strain for SAE 4130 steel heat treated to Rockwell C hardness of 35 (R_C35) were also found in reference 8. Values used for titanium materials properties were the prefabrication as-received values given in reference 4.

The possibility of improving the uniformity of the probability of failure of the failure velocities from reference 4 was investigated. In plots of percent failed versus impact velocity, bimodal and in one case trimodal frequency of failure distributions suggested the presence of more than one heat treatment.

Simonis and Stoneking (ref. 4) indicate that the SAE 4130 hollow steel spheres were heat treated after fabrication. They were austenitized and then tempered to a hardness of R_C35. No range of acceptable hardness was indicated. The spheres were reported as commercially manufactured. When a manufacturing shop works to a specification of "temper to R_C 35," this may be interpreted as the minimum acceptable hardness. In such a case, if the hardness measured after a tempering cycle were R_C40, that hardness would meet the required specification.

Thus, the study of the experimental hollow sphere impact data of Simonis and Stoneking (ref. 4) suggests that variations occurred in the temper hardness and hence in the strength levels of sets of manufactured hollow steel test spheres. Variation in the strengths of sphere materials would contribute to the observed variations in the experimentally measured sphere impact failure velocities.

Cracks, laps, voids, and inclusions resulting from fabrication processes may cause high local stresses to occur during impact and reduce the failure velocity. These factors can be eliminated and/or minimized by careful inspection procedures during and following fabrication.

Equation (7) states that the failure velocity is directly proportional to the square root of $\sigma\epsilon$. The stress, σ, is a stress greater than the yield strength for the sphere material where plastic flow initiates. It is the average true stress on the dynamic true-stress versus true-strain diagram between the yield strength and the rupture strength. This stress when multiplied by the ultimate true strain, ϵ, gives the specific energy for the material in in.-lbf/lbm or Nm/kg. The specific energy is the amount of energy per unit volume absorbed by the material from initial loading to rupture. It is also equal to the area under the dynamic true-stress versus true-strain diagram. Thus, the failure velocity is directly proportional to the square root of the specific energy for the material.

Application of Correlation Equations

The correlation equations presented in this report are strictly applicable only within the ranges of the variables in the hollow sphere impact data listed in Table I. The largest sphere listed in the table is two in. (5.1 cm) in diameter. Application of the equations to larger diameter spheres would constitute an extrapolation. Since the equations may not be applicable outside the ranges of the parameters in the experimental test data used in the analysis, information obtained by extrapolation of the correlation equations must be used with caution.

A sphere with a mean radius to thickness ratio of 2.90 is a thick-walled sphere. Although more data with known material properties and with failure velocities at a definite level of probability are desirable, the available sphere impact test data does cover the range from thin-walled to thick-walled spheres. Limited by the reliability of the available test data, the correlation equations apply over the range of mean radius to thickness ratios represented in the test data.

The failure deformation to mean radius ratio must also be restricted to the range of the test data. At a value of 1.0 the impacted sphere would be deformed to the shape of a hemisphere. This would constitute an extrapolation since the largest experimental value for the ratio is 0.61.

For practical purposes, a containment vessel will contain numerous structural components that will limit the amount of deformation physically possible. After the impact, a containment vessel must also have strength to retain radioactive gases and pressures from the after-heat and melt-down of the reactor. A containment vessel capable of surviving severe damage is very desirable. The impact deformation should be kept small to preserve the post-impact strength of the containment vessel.

In reference 3 it was pointed out that doubling the mean radius to thickness ratio resulted in a small (6 percent) increase in the deformation to mean radius ratio when the parameters were held constant. This observation is based on the small exponent on the ratio R/h in equation (4).

In contrast, the failure deformation to mean radius ratio given by equation (8) is a relatively strong function of the R/h ratio. Equation (7) shows that the failure velocity, V_f, is also strongly dependent on the R/h ratio.

Thus, for a given material, doubling the R/h ratio of a hollow sphere results in only a 6 percent increase in the deformation to mean radius ratio at velocities below the failure velocity, but results in an increase in the failure deformation to mean radius ratio by 56 percent, and an increase in the failure velocity by 47 percent.

Multilayer spheres appear to have advantages over single layer spheres. Consider the impact behavior of two thin-walled spheres. The spheres have the same outside diameter, the same total wall thickness, and are fabricated from the same material. The first has a solid wall. The second has a wall comprised of two layers.

The two spheres are tested at the same impact velocity. Each of the two spherical shells comprising the second sphere with its double wall will absorb part of its own kinetic energy and deform essentially as an individual shell. The mean radius to thickness ratio for each of the two shells comprising the second sphere will be twice that for the first sphere with its solid wall. The deformation of the second sphere will be about six percent greater than the impact deformation of the first.

The second sphere will have important advantages over the first sphere. Stresses and strains resulting from bending of the walls during impact will be reduced. The double layer will can sustain greater deformation during impact without failure. From the above paragraph on doubling the R/h ratio we find that both the deformation and velocity at failure may be increased markedly.

Thus, the equations presented suggest that a multilayer spherical containment vessel may have superior deformation and failure velocity capability compared to a vessel with a solid wall.

Estimate of Failure Velocity for a 17 Foot Diameter Containment Vessel

The purpose of this analysis was to obtain relations for use in the prediction of the failure deformation and failure velocity of a large containment vessel for a nuclear reactor. Application of the correlation equations based on small sphere impact to this large containment vessel constitutes an extrapolation of two orders of magnitude in diameter.

Materials and geometry data are given in figure 7. Deformation-radius ratios are given as a function of impact velocity. The failure deformation-radius ratio for the impact failure velocity is plotted on the graph. The calculated failure deformation-radius ratio from equation (8) is equal to .84, which is greater than 0.61 and hence is outside the range of the expeerimental test data.

The failure velocity of 900 ft/sec (274 m/sec) shown in figure 7 is the value given by equation (7). The vessel impacting at the velocity will have an estimated 50 percent probability of failure.

If the vessel in figure 7 were fabricated with a double wall three inches (7.62 cm) total thickness, the failure deformation-radius ratio and the failure velocity given by the correlation equations would both be increased and those values would be well beyond the range of applicability of the equations. The high values suggest that such a vessel would sustain considerable deformation from an impact velocity greater than 900 feet per second without failure.

CONCLUDING REMARKS

The following conclusions are based on the dimensional analysis of hollow sphere impact test failure data obtained from published references. Failure velocity for a given sphere geometry and material was selected from the limited number of test data points as the lowest impact test velocity that resulted in failure of the sphere. Failure was defined by the presence of a through-crack in the wall of the impacted sphere.

The range of the data is as follows: The failure velocity varied from 297 to 650 ft/sec (91 to 198 m/sec). Sphere geometries ranged from thick-walled to thin-walled spheres. Mean radius to thickness ratios of sphere test data varied from 2.90 to 28.07. Outside diameters ranged from 0.750 to 2.00 inches (1.91 to 5.08 cm). Materials included SAE 4130 steel and titanium spheres tested at room temperature, and Haynes Alloy No. 25 spheres tested at 1800°F (1256°K).

1. Empirical correlation equations given in the report can be used to predict the permanent deformation and the impact velocity which will cause failure of a hollow sphere moving normal to and impacting on a hard flat surface.

2. Thick-walled and thin-walled sphere impact data were correlated with the same equations.

3. The impact deformation which results in failure of the sphere was found to be independent of velocity, density of material, and the ultimate strength of the material.

4. The impact deformation to mean radius ratio (δ_f/R) at failure was found to be a function of mean radius (R), thickness (h), and the ultimate true strain (ϵ).

$$\frac{\delta_f}{R} = 0.109 \left(\frac{R}{h}\right)^{0.64} \epsilon^{\frac{1}{2}}$$

5. The hollow sphere impact failure velocity is a function of mean radius, thickness, ultimate stress (σ), ultimate true strain, and density of the sphere material (ρ).

$$V_f = 0.15 \left(\frac{R}{h}\right)^{0.56} \left(\frac{\sigma}{\rho}\right)^{\frac{1}{2}} \epsilon^{\frac{1}{2}}$$

6. There is a range of velocities between the non-failure level of velocity and the velocity for 100 percent failure. Failure velocity must be defined by specifying the probability of failure. Failure velocities to be compared and correlated must have the same specified probability of failure. Hollow sphere impact test programs are required to provide failure velocity data with a specified probability of failure.

7. Dynamic properties of materials are involved in the impact deformation and failure of hollow spheres. Experimental high strain rate test data is needed for candidate sphere materials. Metal properties required are the dynamic plastic flow stress and the dynamic ultimate true strain.

8. The correlation equations provide a basis for suggesting that a multilayer containment vessel may have superior impact strength compared to a corresponding vessel with a solid wall. Experimental tests are required to investigate this possibility.

9. The correlation equations provided an estimate of V_f = 900 ft/sec for the failure velocity and δ_f/R = .84 for the impact deformation at failure for a large thin-walled containment vessel for a nuclear reactor.

10. Information for the containment vessel obtained by extrapolation of the correlation equations must be used with caution since the equations may not be applicable outside the ranges of the parameters in the experimental test data used in the analysis.

11. Impact tests of large diameter hollow spheres are required to investigate size effects on the impact failure of spheres several feet in diameter compared to the behavior of the small diameter spheres for which experimental test data is available.

12. If large hollow sphere impact tests data correlates with the small sphere impact data, additional small sphere impact tests could provide experimental failure velocities with an equal probability of failure. The new data could then be used to improve the sphere impact deformation and failure velocity correlations for application to the design of large containment vessels.

REFERENCES

1. Rom, Frank E.: Status of the Nuclear Powered Airplane. Journal of Aircraft, Vol. 7, 1970.

2. Puthoff, Richard L.; and Gumto, Klaus H.: Parametric Study of a Frangible-Tube Energy-Absorption System for Protection of a Nuclear Aircraft Reactor. NASA TN D-5730, 1970.

3. Morris, R. E.: Correlation of Small Sphere Impact Deformation Data and Extrapolation to Larger Spheres. NASA TM X-2067, 1970.

4. Simonis, J. C.; and Stoneking, C. E.: A Study of Impact Effects of Spherical Shells. Part II, A Theoretical and Experimental Study of the Response of Spherical Shells to Impact Loads. Rep. SC-CR-67-2540, Sandia Laboratories, Dec. 1966.

5. Haskell, Donald F.: Impact Failure Criterion for Cylindrical and Spherical Shells. The Shock and Vibration Bulletin. Bull. No. 39, Pt. 5, Naval Research Lab., Dec. 1968, pp. 21-27.

6. Anon.: Spherical Capsule Technology Program. Heat Source Technical Report. Rep. HIT-370, Hittman Associates, Inc., Jan. 1969.

7. Johnson, Neil E.: Impact of a Spherical Shell on an Elastic Surface. Ph.D. Thesis, Univ. California, 1967.

8. Weiss, V.; and Sessler, J. G.; eds.: Aerospace Structural Metals Handbook. Vol. I: Ferrous Alloys. Syracuse University Press, 1963.

TABLE I

Impact Failure Test Data for Spherical Shells

Symbol	Material[a]	O.D.		I.D.		Wall Thickness h		R/h	Failure Velocity V_f		Deflection δ		Symbol[b]
		in.	cm.	in.	cm.	in.	cm.		fps	m/sec	in.	cm.	
○	1	1.000	2.54	.860	2.18	.070	.178	6.64	650	198	.203	.052	4
□	1	.823	2.09	.665	1.69	.079	.201	4.71	389	119	.107	.027	4
⬡	1	1.177	2.99	1.019	2.59	.079	.201	6.95	454	138	.183	.046	4
▽	1	1.250	3.18	1.050	2.67	.100	.254	5.75	297	91	.134	.034	4
◇	1	1.000	2.54	.800	2.03	.100	.254	4.50	358	109	.118	.030	4
⬠	1	1.177	2.99	.935	2.37	.121	.307	4.36	307	94	.123	.031	4
△	1	1.000	2.54	.730	1.85	.130	.330	3.35	346	105	.107	.027	4
▱	1	.750	1.91	.550	1.40	.100	.254	3.25	307	94	.072	.018	4
◇	1	.823	2.09	.581	1.48	.121	.307	2.90	350	107	.082	.021	4
◇	2	1.000	2.54	.800	2.03	.100	.254	4.50	397	121	.082	.021	4
▷	3	2.000	5.08	1.930	4.90	.035	.089	28.07	390	119	.598	1.519	6

a. Materials

1. SAE 4130 Steel
2. Titanium
3. Haynes Alloy No. 25

b. Source of Test Data (Reference No.)

TABLE II

Sphere Materials

Material	Ultimate Strength, σ KSI	Ultimate Strength, σ MN/m^2	Ultimate True Strain, ϵ	Density, ρ lb/in^3	Density, ρ g/cm^3	Remarks
SAE 4130 Steel	143	986	.75	.283	7.83	Data for 0.040 inch (1.02 mm) sheet 1570°F (1128°K) OQ, 1000°F (811°K) - 2 hr, R_C 33-35, Ref. 8.
Titanium	99	774	.62	.163	4.51	Ref. 4, BHN 221, as received.
Haynes Alloy No. 25	27	186	.43	.330	9.13	Refs. 6 and 8. Aged 500 hrs. at 1500°F (1089°K), tested at 1800°F (1256°K).

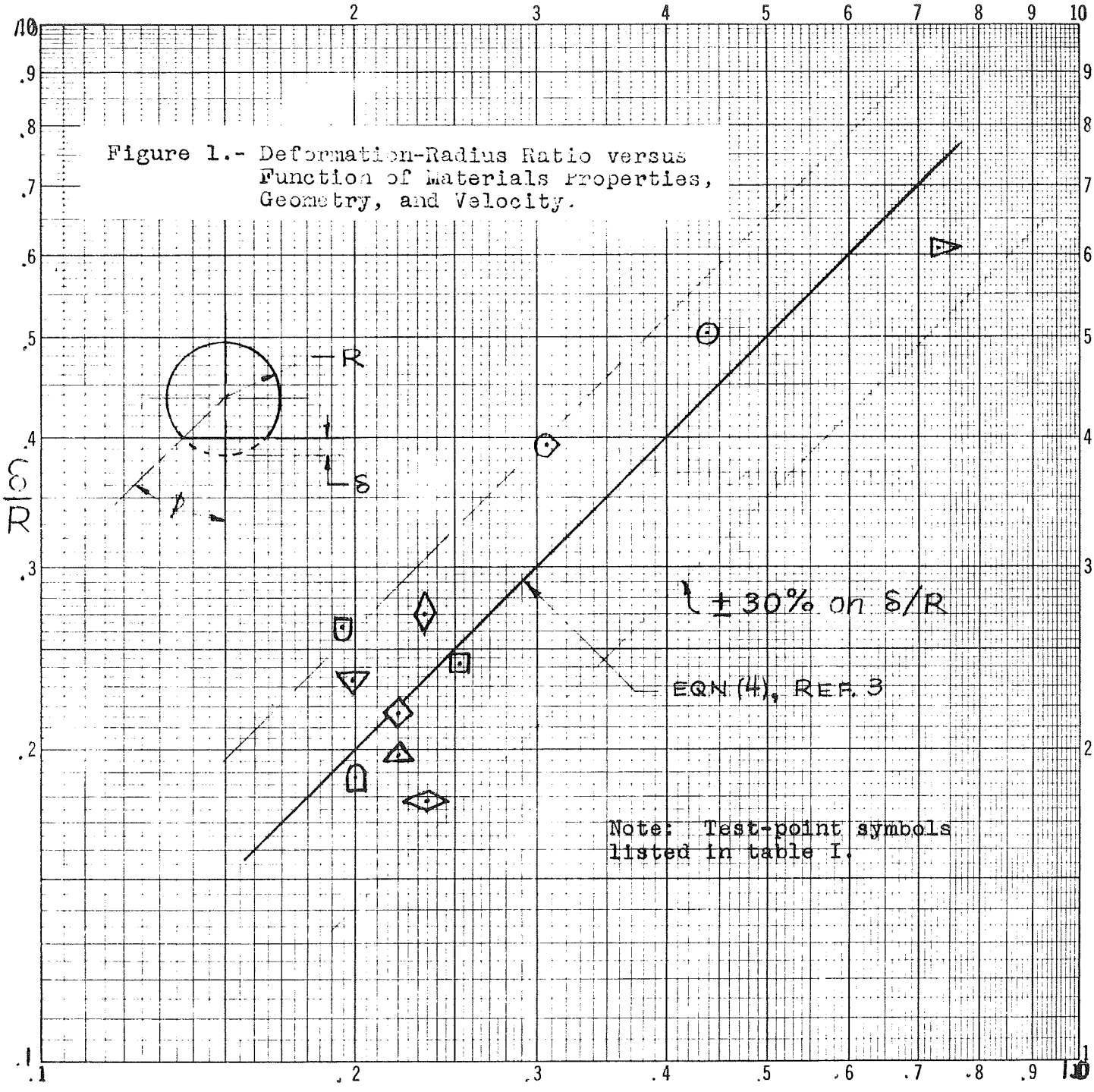
Figure 1.- Deformation-Radius Ratio versus Function of Materials Properties, Geometry, and Velocity.
δ/R
R
δ
h
± 30% on δ/R
EQN (4), REF. 3
Note: Test-point symbols listed in table I.
0.67 $\left(\frac{\rho V^2}{\sigma}\right)^{\frac{1}{2}}\left(\frac{R}{h}\right)^{.08}$

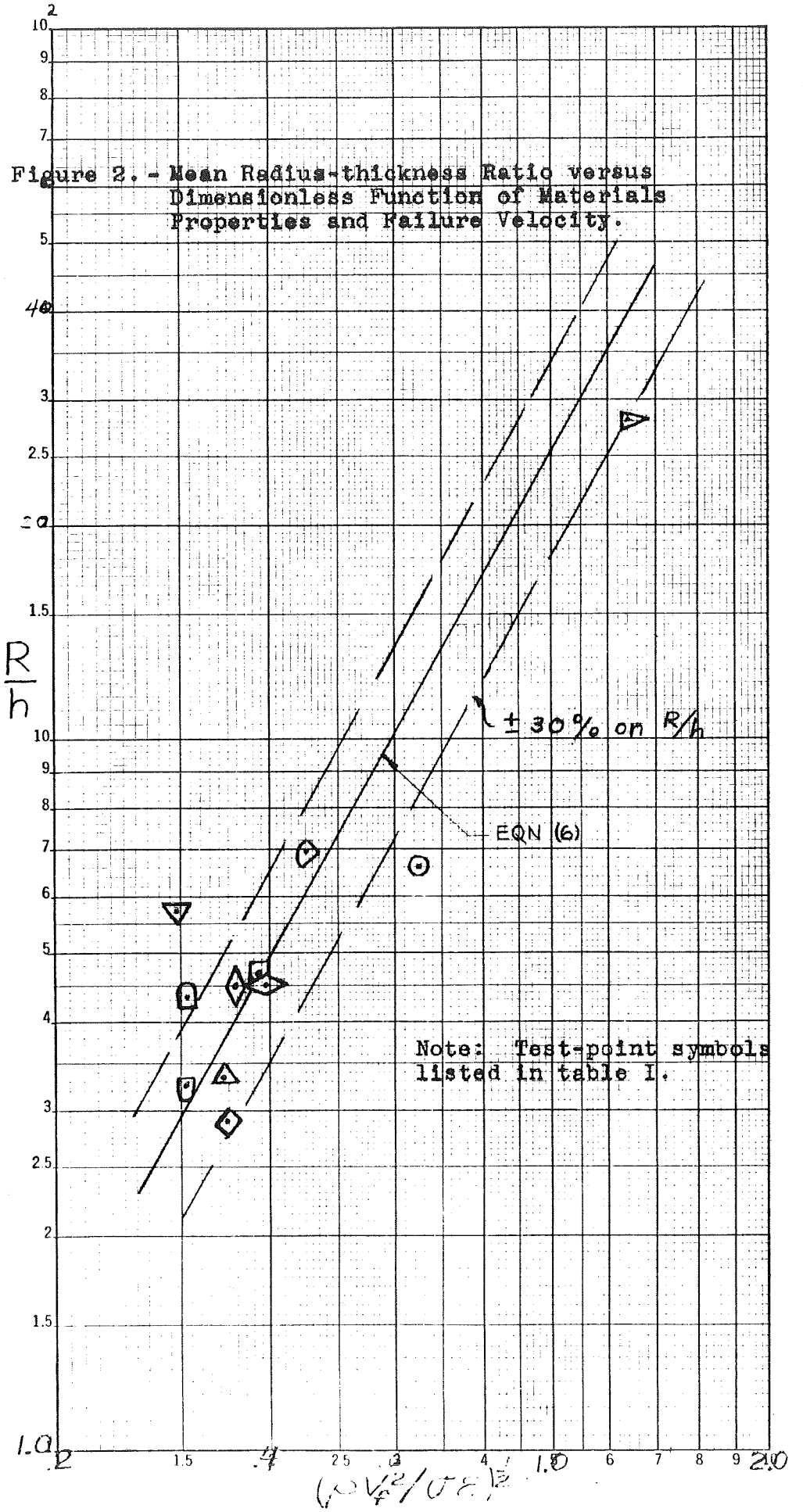

Figure 2. - Mean Radius-thickness Ratio versus Dimensionless Function of Materials Properties and Failure Velocity.

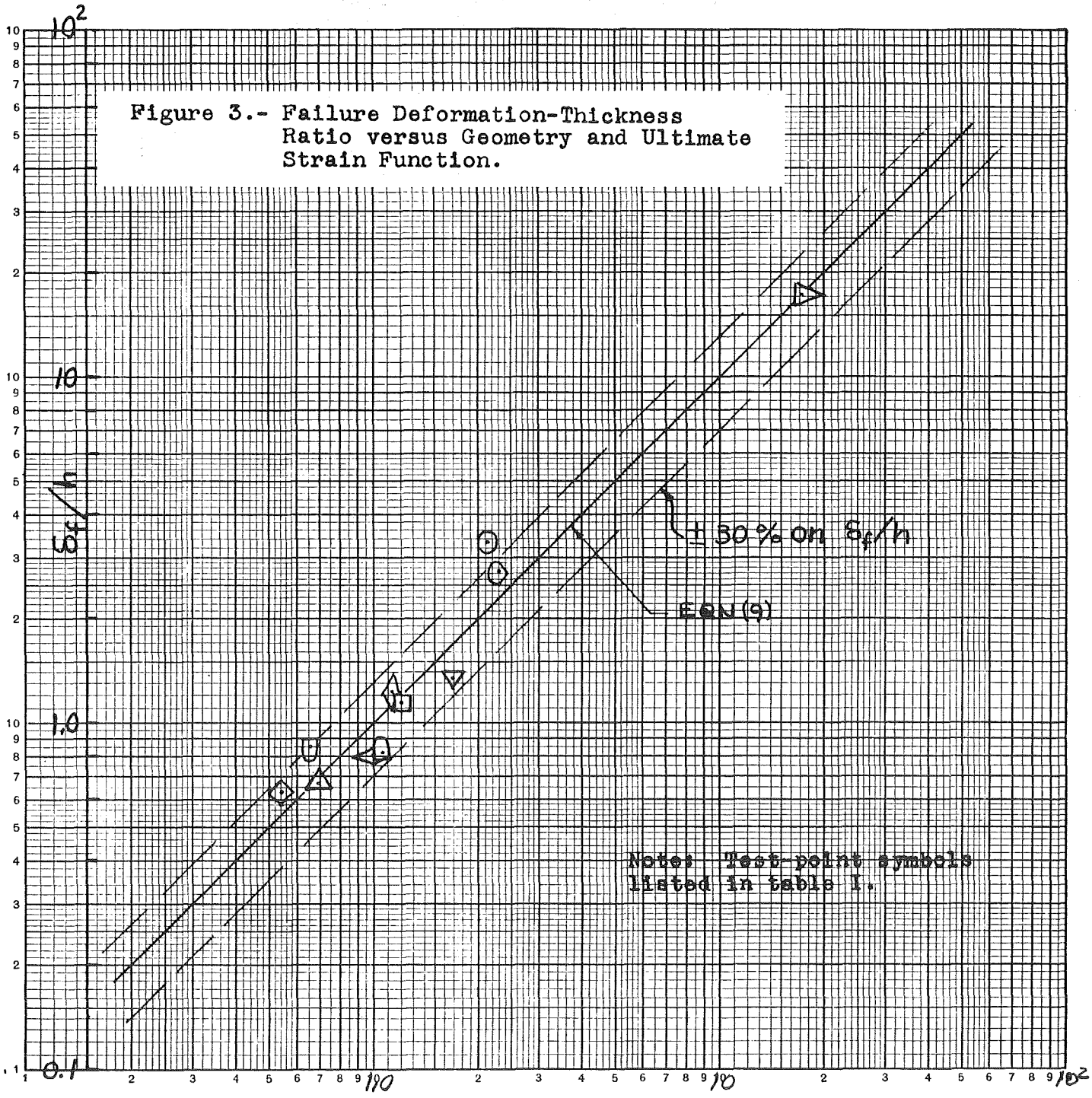

Figure 3.- Failure Deformation-Thickness Ratio versus Geometry and Ultimate Strain Function.

$$0.109 \left(\frac{R}{h}\right)^{1.64} \varepsilon^{\frac{1}{2}}$$

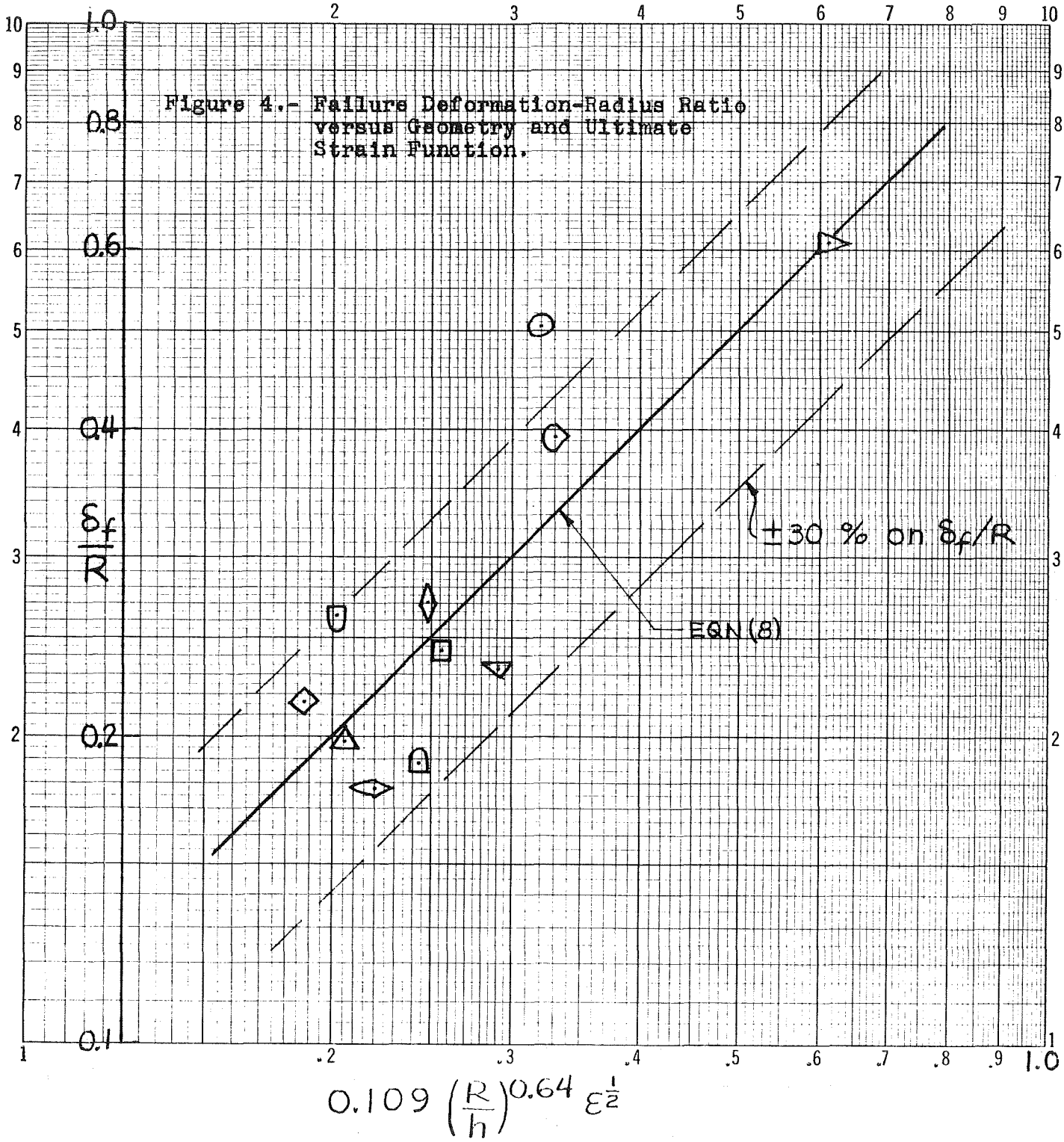
Figure 4.- Failure Deformation-Radius Ratio versus Geometry and Ultimate Strain Function.
$\frac{\delta_f}{R}$
$0.109 \left(\frac{R}{h}\right)^{0.64} \varepsilon^{\frac{1}{2}}$
±30 % on δ_f/R
EQN (8)
1.0
0.8
0.6
0.4
0.2
0.1

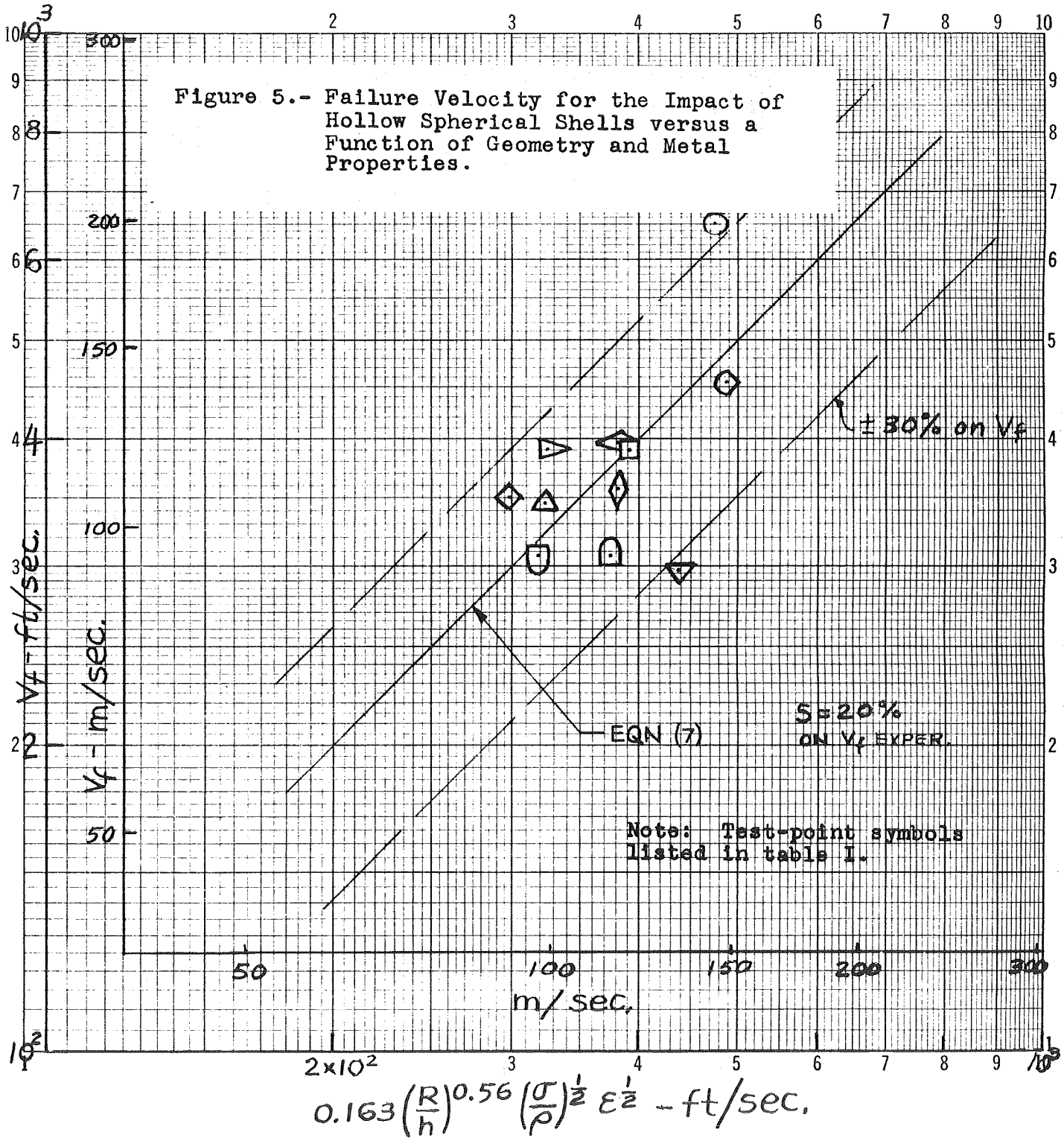
Figure 5.- Failure Velocity for the Impact of Hollow Spherical Shells versus a Function of Geometry and Metal Properties.
V_f - ft/sec.
V_f - m/sec.
± 30% on V_f
EQN (7)
S = 20% ON V_f EXPER.
Note: Test-point symbols listed in table I.
m/sec.
$0.163\left(\frac{R}{h}\right)^{0.56}\left(\frac{\sigma}{\rho}\right)^{\frac{1}{2}}\varepsilon^{\frac{1}{2}}$ - ft/sec.

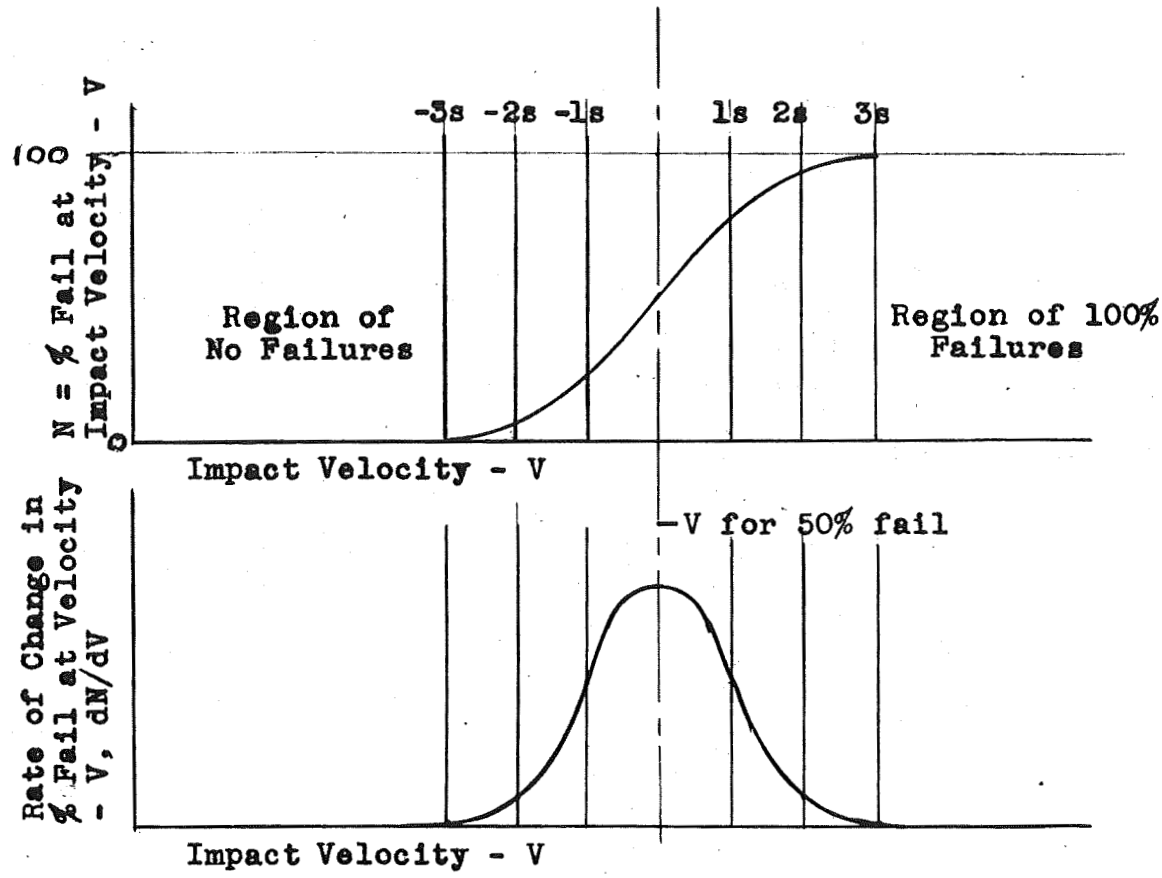

Figure 6. - Variation of Per cent Failures as a Function of Impact Velocity.

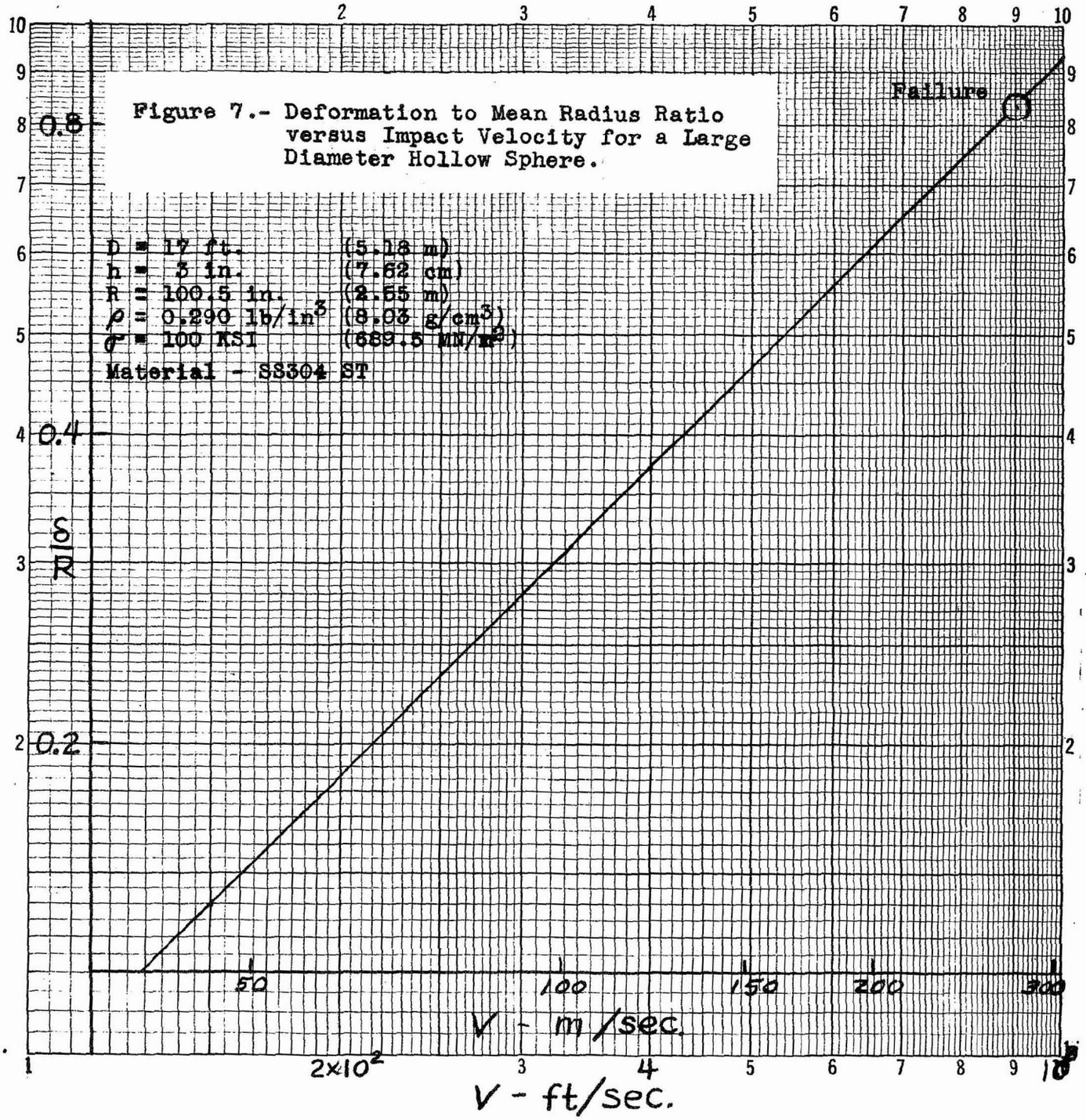

Figure 7.- Deformation to Mean Radius Ratio versus Impact Velocity for a Large Diameter Hollow Sphere.